Int J Clin Exp Pathol 2019;12(6):1975-1991
www.ijcep.com /ISSN:1936-2625/IJCEP0092976

Original Article

The effects of a graded increase in chronic hypoxia exposure duration on healthy rats at high-altitude

Wei Cai[1,2,3*], Ziquan Liu[2*], Guangzong Li[3], Peixin Xiao[4], Qi Lv[2], Yanhua Gong[2], Haojun Fan[2], Shike Hou[2], Hui Ding[2]

[1]Logistics University of Chinese People's Armed Police Forces, Tianjin, China; [2]School of Disaster Medical Research, Tianjin University, Tianjin, China; [3]Chinese People's Armed Police Force (PAP) Medical Center, Tianjin, China; [4]Hubei Provincial Corps Hospital, Chinese People's Armed Police Forces, Wuhan, China. [*]Equal contributors and co-first authors.

Received February 24, 2019; Accepted March 27, 2019; Epub June 1, 2019; Published June 15, 2019

Abstract: To investigate the effects of chronic hypoxia exposure at high altitude on the formation of pulmonary edema in rats, we randomized rats into normoxic control groups and hypoxic 24, 48, and 72-hour exposure groups. In the hypoxic exposure group, the arterial blood gas, wet-dry weight ratio (W/D), lung tissue permeability index (LPI), bronchoalveolar lavage fluid (BALF) and plasma levels of the inflammatory factors were measured after continuous, chronic hypoxic exposure for a corresponding time, and the pathological changes in the lung tissue and the expression of tight junction-associated protein occludin were observed. We found that the contents of arterial blood gas, W/D, LPI, BALF and plasma IL-6, TNF-α, and IL-10 in the hypoxic exposure group were significantly different from the contents of arterial blood gas in the normoxic control group. H&E staining showed tissue effusion, a marked thickening of the pulmonary septum, interstitial inflammatory cells, and erythrocytic infiltration. Compared with the normoxic control group, the pulmonary edema score was significantly increased in the hypoxic 48-hour group. Toluidine blue staining showed that the mast cell count and degranulation rate were significantly increased in the hypoxic 48-hour and 72-hour groups, but massone staining showed no significant pulmonary interstitial fibrosis in the 4 groups. Occludin expression was significantly higher in the normoxic control group than it was in the hypoxic exposure group. These results indicated that different chronic hypoxic exposure durations at the plateau all caused high-altitude pulmonary edema in rats, but there was no significant difference in some indicators among the groups.

Keywords: High-altitude pulmonary edema, hypoxic exposure duration, digital animal experiment room

Introduction

As the pulmonary manifestation of acute altitude disease, high-altitude pulmonary edema (HAPE) is a serious life-threatening, non-cardiogenic pulmonary edema with hydrostatic characteristics [1, 2]. HAPE occurs when people who quickly rise to more than 2,500 metres above sea level do not adapt to the plateau environment [3]. HAPE is a potentially fatal altitude sickness and the most common cause of death in altitude sickness [4]. HAPE rarely occurs after a week or a few weeks of acclimation at a specific altitude. However, studies have reported that HAPE will occur when local plateau residents who have been acclimated at a certain altitude for a period of time are re-exposed to the hypoxic environment, indicating that the acclimation at the plateau shows regional and population differences [5].

In recent years, studies on HAPE have mainly focused on single nucleotide polymorphism-related genes in susceptible populations, subclinical symptoms and important diagnostic markers, but basic experimental animal studies on the pathogenesis of HAPE are limited [6-8]. Currently, animal HAPE models can be divided into three types [9, 10]. The first model type places the animal on a treadmill while moving in a low-pressure, low-oxygen environment for a certain period of time. The second model type places the animals in an environment where oxygen is normally depressed and replaces oxygen in the air with a mixture of gases, such as nitrogen, simulating the hypoxic environment

and observing the changes in the animals (such as pigs) at the same time. The third model type places the animal in a low pressure oxygen chamber and observes the corresponding changes over time. The first two models use time as a control variable to observe the changes in the animal indicators, while the third model mainly reflects the impact of time changes on the experimental animals. Existing animal models of HAPE include rabbits, goats, dogs, pigs and ferrets, but these animal choices are not sustainable or repeatable due to limitations, such as laboratory conditions [11]. Although none of the models are ideal animal models, most physiological studies of altitude sickness have used rat models. Rats have been shown to induce a hypoxic pulmonary vasoconstriction response (HPVR) under hypoxic conditions, leading to the occurrence of pulmonary edema, and a HAPE susceptible population is also closely related to HPVR. When exposed to a low-pressure and hypoxic environment, excessive HPVR induces the occurrence of HAPE [12, 13]. Studies have also shown that HAPE susceptibility in rats may also be associated with upper respiratory tract infection [14]. However, most of the current rat models lack a continuous observation of the initial onset of HAPE in the simulated high-altitude environment within a few days. In our model, the occurrence of HAPE in rats exposed to high altitude, namely, hypobaric hypoxic conditions of 24 hours, 48 hours, and 72 hours, was simulated by a special low-pressure hypoxic chamber. The changes in the lungs, and specific indexes in the rats at different altitudes were compared, and a stable experimental HAPE model was demonstrated in these animal experiments.

Rapid ascension and individual susceptibility are two important factors that cause HAPE [15, 16]. In this experiment, we used a digital animal experimental cabin to simulate an increase to an altitude of 6000 metres at a rate of 10 m/s, and we continued to maintain the plateau pulmonary edema in animals at the simulated high altitudes. At 24, 48, and 72 hours, the experimental groups were hypothesized to have had symptoms related to HAPE. By analysing the changes of the relevant indexes in the normoxic control group and the hypoxic exposure group, the objective changes in the laboratory lung tissue indexes in the early stages of high-altitude pulmonary edema were explored.

Materials and methods

Experimental animals

SPF grade adult male SD rats, weighing 180-200 g, were purchased from the animal center of the academy of military medical sciences, with the production license number of SCXK (army) 2014-0013. All the rats were exposed to temperatures in advance from 20 to 28°C, humidity 40-70% in an indoor environment for two days. All animal experiments were approved by the animal ethics committee of the Chinese People's Armed Police Force (PAP) Medical Center. All animal experiments were conducted in accordance with the Helsinki convention and the guidelines for the care and use of laboratory animals.

Animal model

Forty SD rats were randomly divided into four groups: the normoxic control group (n = 10) and three hypoxic exposure groups (n = 30). Three hypoxic exposure groups were divided into the low pressure, low oxygen, and low temperature exposure groups (24, 48, and 72 hours) (n = 10). During the experiments, the hatch was opened, and the animals from the hypoxic exposure group were placed in the cabin (**Figure 1A**, **1B**). After confirming the placement using the external display, the door was closed using manual bolts, and the equipment power supply was started and the low-pressure and low-oxygen parameters were set. The altitude was set at 6000 meters, the time was set according to the appropriate group condition, the pump operating time was 720 min, the rate of altitude change was 10 m/s, and the temperature was set to 10°C. The refrigeration mode was started. After the equipment achieved the pre-set altitude, the cabin temperature was maintained at (10 ± 1)°C, the humidity was maintained at (60 ± 10)%, the cabin pressure was 54.5 KPa, and the oxygen partial pressure was 9.9 KPa. After each modeling, the touch screen showed that the simulated altitude automatically drops. After the height was lowered to the safe height, the hatch was opened again, and the animal was quickly anesthetized in the cabin, and the abdominal aortic blood was immediately taken (**Figure 1C**).

Sample anatomy and collection

Rats in each group were injected intraperitoneally with 2% pentobarbital (2 ml/0.1 kg) and fix-

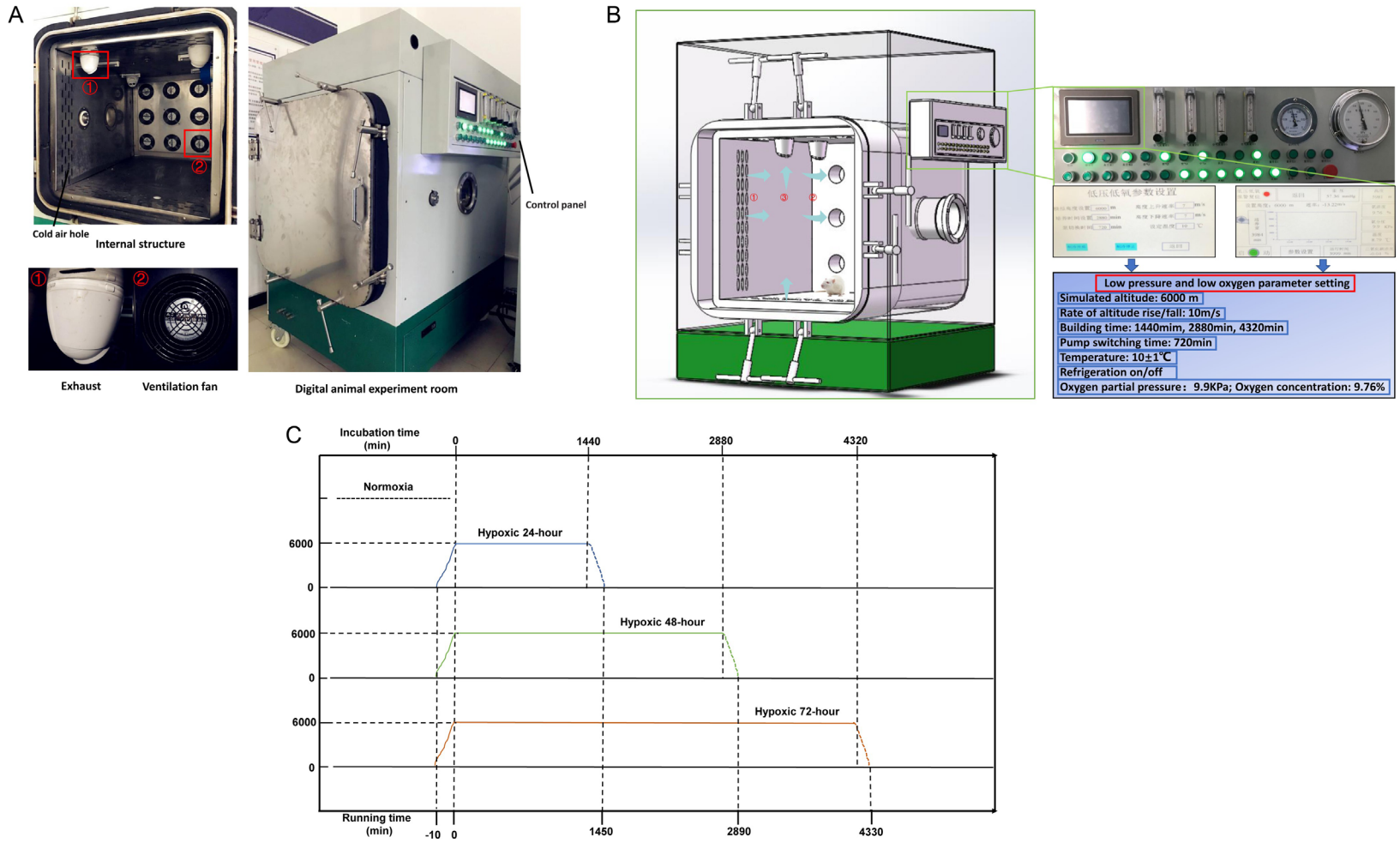

Figure 1. Digital animal experiment room. A. The digital animal experiment room is composed of three parts: the control instrument panel outside the module and the animal module inside the module. ① Low pressure pump, used to simulate the state of low pressure in the plateau; ② Exhaust fan, used for gas exchange in the cabin. After starting the cooling hole, the low temperature environment in the cabin can be maintained. B. Schematic diagram of digital animal experiment room. ① The cold air flows out from the cooling hole; ② Air exchange direction; ③ Low pressure pump suction air direction. C. Time-height curve can be divided into three sections: The first section is the uniform rising section, with the speed of 10 m/s rising to the altitude of 6000 meters; The second stage is the molding stage, and the height remains unchanged. The third stage is a constant falling stage, with a rate of decline of about 10 m/s. After falling to a safe height, it stops falling.

ed in a supine position. A longitudinal incision was made in the middle of the abdomen above the perineum. After the abdominal cavity was fully exposed, 2 ml of arterial blood was drawn from the abdominal aorta, and the blood sample was immediately dropped into a blood gas analyser for arterial blood gas analysis. The thoracic cavity was opened, and a ligature was placed around the right main bronchus. Through a tracheal intubation, 4 ml of 0.9% normal saline was slowly injected into the left lung through the left main bronchus, and the saline was slowly withdrawn and re-injected; this rinsing was repeated 2-3 times. The alveolar lavage was collected, the solution was centrifuged at 800 g for 10 minutes at 4°C, and the supernatant was retained. The right lung was separated, and the right upper lobe was used to measure the W/D. The right middle lobe was fixed using 4% paraformaldehyde, and the lower right lobe was stored in a low-temperature freezer at -80°C.

Arterial blood gas

Arterial blood pH, arterial blood carbon dioxide partial pressure ($PaCO_2$), arterial oxygen partial pressure (PaO_2), arterial oxygen saturation (SaO_2) bicarbonate concentration in plasma (HCO_3), total carbon dioxide in plasma (TCO_2) and base Excess Extracellular Fluid (BEecf) were analysed using the iSTAT-200 Portable Clinical Blood Gas Analyzer (Abbott, Illinois, USA).

Wet-to-dry weight ratio (W/D)

The blood-contaminated upper right lobe was washed with 0.9% NaCl, and the excess moisture on the surface of the tissue was gently blotted using a clean gauze strip. The lobe was then placed on foil, and the wet weight was measured using an electronic balance. The tissue was then placed, together with the foil, in an electric oven. The mixture was heated at 60°C for 48 hours, and subsequently the weight was recorded as the dry weight. W/D was calculated to evaluate the lung tissue edema.

Lung permeability index (LPI)

Depending on the amount of the standard and the sample, 1 volume of copper reagent and 50 volumes of BCA reagent were mixed. The BCA working solution was prepared and mixed well. Then, 10 μl of the BSA standard was diluted to 100 μl with PBS to give a final concentration of 0.5 mg/mL, and 0, 2, 4, 6, 8, 12, 16, 20 μl of the standard was added to the wells of a 96-well plate. The diluted standard was added to 20 μl of the sample to be tested. Then, 20 μl of the diluted sample was added to the 96-well plate, and 200 μl of the BCA working solution was added to each well. The plate was held at 37°C for 30 min. The absorbance at 562 nm was measured using an ultra-micro UV spectrophotometer (IMPLEN, NanoPhotometer NP80 Mobile, GER). BALF and plasma total protein content were measured according to the standard curve. LPI = Total BALF protein concentration/Total plasma protein concentration.

Measurements of IL-6, TNF-α and IL-10 levels in plasma and BALF

The plasma and bronchoalveolar lavage fluid samples were analyzed using an ELISA kit (Nanjing, completed at the Institute of Bioengineering, China) according to the instructions, and IL-6, TNF-α, IL-10, and other inflammatory factors were analyzed.

Histopathological staining

H&E staining and lung injury score: After the right middle lobe of each lung was fixed in 4% paraformaldehyde for 48 h, the tissue was cut into tissue pieces that were approximately 5 mm × 5 mm × 5 mm, placed in a grid trough, dehydrated by gradient ethanol, made transparent in xylene, embedded in paraffin, serial sectioned, stained with H&E, and packed with neutral gum. Then, eight different fields were randomly selected from the control group and the hypoxic exposure group. The lung tissue structure, lung septum, and red blood cell exudation were observed under light microscopy. Inflammatory cell infiltration and pulmonary edema images were collected and pathologically scored. The severity of lung injury was based on the following scoring criteria: no damage = 0 points; 25% injury area = 1 point; 50% injury area = 2 points; 75% injury area = 3 points; total lung injury = 4 points [17]. Two pathologists observed and scored the extent of lung tissue damage using the double-blind method.

Toluidine blue staining and mast cell count in lung tissue: The modified toluidine blue staining

method was used. Under observation by a biological inverted microscope (DMI3000B; Leica, Wetzlar Germany), ten high-power fields (× 400) were randomly selected to count the number of mast cells and to count the degranulation rate of the mast cells.

MC degranulation rate = MC degranulation number/total number of MC × 100%.

Masson staining: After routine dewaxing in water, the tissues were stained using a Masson staining kit (Solarbio, Beijing, China) according to the manufacturer's instructions. Six different fields of view were randomly selected from the biological inverted microscope (DMI3000B; Leica, Wetzlar Germany) to observe the lung tissue structure, lung interval and pulmonary interstitial fibrosis.

Tight junction related protein (occludin): The expression of the tight junction-associated protein occludin was detected by immunohistochemistry using a rabbit anti-mouse Occludin monoclonal antibody (Abeam). The mean optical densities (MOD) of five lung tissue sections in the control and plateau pulmonary edema groups were measured using the Image-Pro Plus 6.0 image processing system to quantify the expression of occludin.

Statistical method: Statistical analyses was performed using SPSS 20.0. All data are expressed as the mean ± standard deviation (SD). One-way analysis of variance was used for comparisons between groups. The LSD test was used for comparisons between groups. The Dunnett T3 test was used when the variance was not uniform. $P < 0.05$ was considered to be statistically significant.

Results

General condition of the rats

All the rats in the experimental group survived during the testing process. Among them, the rats in the normoxia control group were active, and the vigour of the rats in the hypoxic exposure group decreased with an increase in the altitude and a decrease in the cabin temperature and oxygen content. In the hypoxic exposure group, the abdominal aorta blood was dark red; in the normoxic control group, the abdominal aorta blood was bright red.

Gross morphological changes in the lung tissue

The thoracic cavity of the rats in each group was exposed, and the left lung was observed. The lung surface of the normoxic control group was pale pink, soft and smooth in texture, had sharp edges, and no obvious bleeding or exudation (**Figure 2A**). In the hypoxic exposure group, the lungs of the rats had different degrees of bleeding and exudation. Among them, a small number of bleeding spots were observed on the surface of the lungs in the 24-hour hypoxia group, and the edges were relatively round and blunt (**Figure 2B**). In the 48-hour hypoxia group, the lungs showed scattered bleeding spots and dark red ecchymoses, and the lung surface was red and white (**Figure 2C**). In the 72-hour hypoxia group, the rats showed obvious dark purple large ecchymoses, and the lung exudation was heavier than the normoxic control group (**Figure 2D**). The percentage of visible lung injury area increased with the increase of modeling time (**Figure 2E**), and the visible lung injury rate also increased with the increase of modeling time (**Figure 2F**).

Percentage of damaged lung tissue area = damaged lung area/ipsilateral lung area × 100%; Lung tissue injury rate = the number of macroscopically visible rats/the number of rats in each group model × 100%.

Arterial blood gas analysis

Compared with the normoxic control group, PaO_2 and SaO_2 in the 24-, 48-, and 72-hour hypoxia groups were significantly lower ($P < 0.01$), but $PaCO_2$ and the pH were not significantly different. In the hypoxic exposure group, the PaO_2 and SaO_2 in the 72-hour hypoxia group were significantly lower than they were in the hypoxic 24-hour group ($P < 0.01$). Compared with the 48-hour hypoxia group, the PaO_2 in the 72 h hypoxia group was significantly decreased ($P < 0.05$). SaO_2 also decreased significantly ($P < 0.01$). TCO_2, HCO_3 and BEecf are indicators of acid-base metabolism. Compared with the normoxic control group, TCO_2 and BEecf were significantly lower in the 24-hour hypoxia group ($P < 0.01$), and HCO_3 was also significantly lower ($P < 0.05$). TCO_2, HCO_3 and BEecf in the 48- and 72-hour hypoxia groups decreased significantly ($P < 0.01$). In the hypoxic exposure group, compared with the 24-hour hypoxia group, the TCO_2

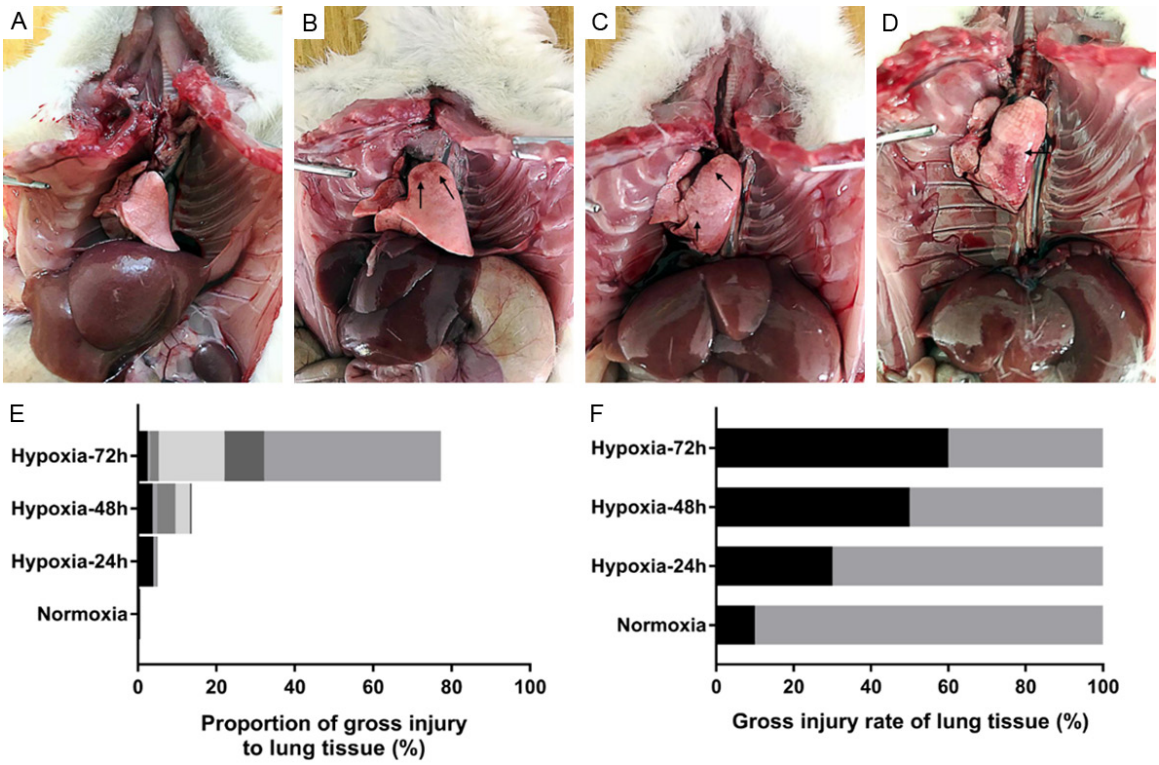

Figure 2. Macroscopic view of rat lung tissue. A. Normoxic control group; B. Hypoxic 24-hour group, arrow indicates small bleeding point; C. Hypoxia 48-hour group, arrow indicates small bleeding point and scattered ecchymosis; D. Hypoxia 72-hour group, the arrow refers to a large area of freckle. E. Proportion of gross injury to lung tissue in each group. Different colors show the proportion of each group of samples. F. Gross injury rate of lung tissue shows the proportion of visible damage samples in the total number of each group.

in the 72-hour hypoxia group was significantly lower ($P < 0.05$), and the HCO_3 and BEecf were also significantly lower ($P < 0.01$); compared with the hypoxic 48 hour group, TCO_2, HCO_3 and BEecf were significantly lower in the 72-hour hypoxia group ($P < 0.01$) (**Table 1**).

Analysis of W/D and LPI of lung tissue

Compared with the normoxic control group, W/D and LPI were significantly increased in the hypoxic 24-hour group ($P < 0.05$), W/D and LPI were significantly increased in the hypoxic 48-hour and 72-hour groups ($P < 0.01$). In the hypoxic exposure group, W/D was significantly increased in the 48-hour hypoxia group compared with the 24-hour hypoxia group ($P < 0.05$) (**Figure 3**).

Levels of IL-6, TNF-α, and IL-10 in BALF and plasma

As shown in **Figure 4**, compared with the normoxic control group, the levels of IL-6 in the plasma and BALF were significantly increased in the hypoxic 24, 48, and 72-hour groups ($P < 0.01$) (**Figure 4A**, **4D**), and were highest after 48 hours of hypoxic exposure. The levels of TNF-α in the plasma and BALF were significantly higher than they were in the normoxic control group at 24, 48, and 72 h after hypoxic exposure ($P < 0.01$) (**Figure 4B**, **4E**). The content of TNF-α in the plasma was the highest at 48 h after hypoxic exposure, showing the same change trend as IL-6. The levels of IL-10 in the plasma and BALF were significantly increased in the hypoxic 24, 48, and 72-hour groups, with a gradient increase ($P < 0.01$) (**Figure 4C**, **4F**). The levels of Il-6 in the plasma and BALF were significantly increased in the hypoxic group at 48 h ($P < 0.01$) compared with the hypoxic group at 24 h ($P < 0.05$), and significantly increased in the hypoxic group at 72 h ($P < 0.05$; $P < 0.01$) (**Figure 4A**, **4D**). Il-6 was also significantly increased in the plasma and BALF at 72 h compared to the hypoxic group ($P < 0.01$) (**Figure 4A**, **4D**). After 48 and 72 h of

Table 1. Analysis of arterial blood gases in four groups of rats (n = 10, $\bar{x} \pm s$)

Group	PO_2 (mmHg)	PCO_2 (mmHg)	PH	SaO_2 (%)	TCO_2 (mmol/L)	HCO_3 (mmol/L)	BEecf (mmol/L)
Normal oxygen control group	90.50 ± 8.22	43.59 ± 6.60	7.36 ± 0.07	95.80 ± 1.81	28.40 ± 1.51	25.83 ± 1.29	0.90 ± 0.88
Hypoxia 24-hour group	67.40 ± 9.86[b]	40.87 ± 14.23	7.38 ± 0.07	90.00 ± 3.09[b]	22.60 ± 3.69[b]	23.35 ± 3.06[a]	2.00 ± 1.94[b]
Hypoxia 48-hour group	64.80 ± 6.61[b]	42.43 ± 7.15	7.39 ± 0.02	86.40 ± 4.06[b]	22.70 ± 2.71[b]	21.61 ± 2.50[b]	4.00 ± 2.11[b,c]
Hypoxia 72-hour group	55.00 ± 8.60[b,d,e]	42.18 ± 13.19	7.34 ± 0.06	73.50 ± 8.48[b,d,f]	19.40 ± 2.07[b,c,f]	18.29 ± 1.89[b,d,f]	7.60 ± 1.84[b,d,f]

Compared with the normoxic control group, [a]$P < 0.05$, [b]$P < 0.01$; compared with the hypoxic 24-hour group, [c]$P < 0.05$, [d]$P < 0.01$; compared with the hypoxic 48-hour group, [e]$P < 0.05$, [f]$P < 0.01$.

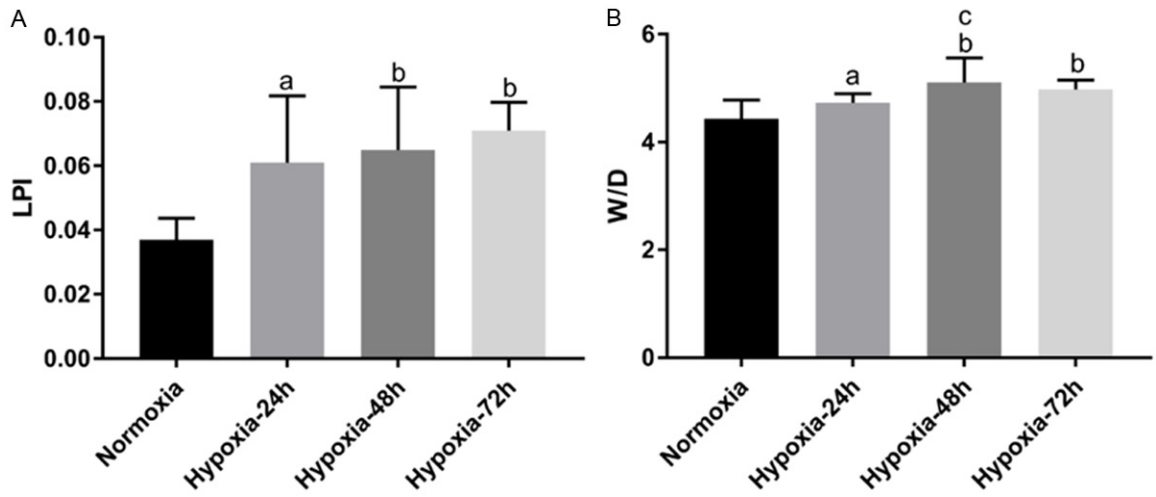

Figure 3. W/D and LPI of lung tissue in rats. Compared with the normoxic control group, [a]P < 0.05, [b]P < 0.01; Compared with the hypoxic 24-hour group, [c]P < 0.05.

hypoxic exposure, the levels of TNF-α in the plasma and BALF were significantly higher than they were in the hypoxic 24-hour group (P < 0.01) (**Figure 4B**, **4E**). The content of TNF-α in the plasma was also significantly higher than it was in the hypoxic group at 72 h after hypoxic exposure (P < 0.05) (**Figure 4B**). The levels of IL-10 in plasma and BALF were significantly increased in the hypoxic group at 48 and 72 hours (P < 0.01) (**Figure 4C**, **4F**) compared with the hypoxic group at 24 hours, and the contents of IL-10 in the plasma and BALF were also significantly increased in the hypoxic group at 72 hours (P < 0.05; P < 0.01) (**Figure 4C**, **4F**).

Pathological changes in the lung tissue

H&E staining of the rat lung tissue showed that the alveolar structure was intact in the normoxic control group, the pulmonary septum was basically not thickened, no obvious edema was observed in alveolar cavity or the lung interstitium, erythrocyte distribution was observed in alveolar and lung interstitium, and there was no significant difference in neutrophil or macrophage infiltration between the normoxic control group and the hypoxic exposure group. Compared with the normoxic control group, the hypoxic exposure group showed a different degree of lung tissue structure damage, characterized by alveolar damage of structural integrity, alveolar cavities expanding in mutual fusion, lung interval clearly thickening, alveolar space and pulmonary interstitial edema showing a visible light pink liquid, edema fluid in the visible red blood cells and inflammatory cells, red blood cells infiltrating extensively (**Figure 5A**). There was no significant difference in the degree of pathological lung tissue damage among the three hypoxic exposure groups. The lung tissue injury scores are shown in **Figure 5A**. Compared with the normoxic control group, the inflammatory score was significantly reduced in the hypoxic 24-hour group (P < 0.05), while the score was increased in the hypoxic 48-hour group and 72-hour group, but there was no significant difference (P > 0.05) (**Figure 5Ae**). Compared with the hypoxic 24-hour group, the inflammation score of the hypoxic 48-hour group was significantly increased (P < 0.05) (**Figure 5Ae**). The hemorrhage score was significantly increased in the 72-hour hypoxic group and was also increased in the 48-hour hypoxic group, but there was no significant difference (P > 0.05) (**Figure 5Af**). Compared with the hypoxic 24-hour group, the hemorrhage score of the hypoxic 72-hour group was significantly increased (P < 0.01) (**Figure 5Af**). The edema score was significantly increased in the hypoxic 48-hour group (P < 0.05), and the hypoxic 72-hour group was also elevated, but there was no significant difference (P > 0.05) (**Figure 5Ag**). Compared with the hypoxic 24-hour group, the edema score of the hypoxic 48-hour group was significantly increased (P < 0.05) (**Figure 5Ag**). The total score was significantly increased in the hypoxic 48-hour group (P < 0.05), while it was increased in the hypoxic 72-hour group, but there was no significant difference (P > 0.05) (**Figure 5Ah**). Compared with

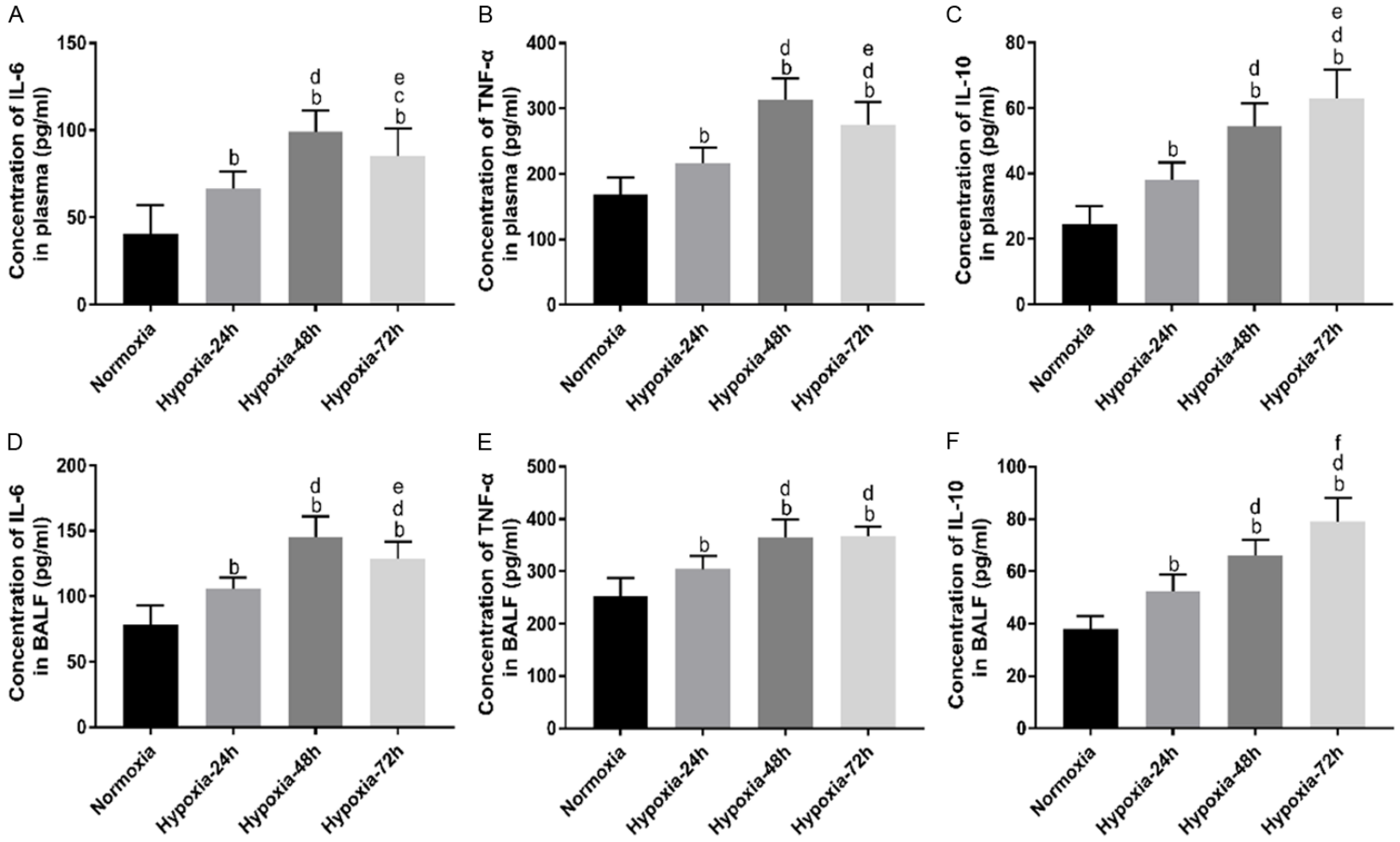

Figure 4. The levels of IL-6, TNF-α and IL-10 in plasma and BALF. The concentrations of IL-6, TNF-α and IL-10 in plasma and BALF were measured by ELISA. Compared with the normoxic control group, $^{a}P < 0.05$, $^{b}P < 0.01$; Compared with the hypoxic 24-hour group, $^{c}P < 0.05$, $^{d}P < 0.01$; Compared with the hypoxic 48-hour group, $^{e}P < 0.05$, $^{f}P < 0.01$.

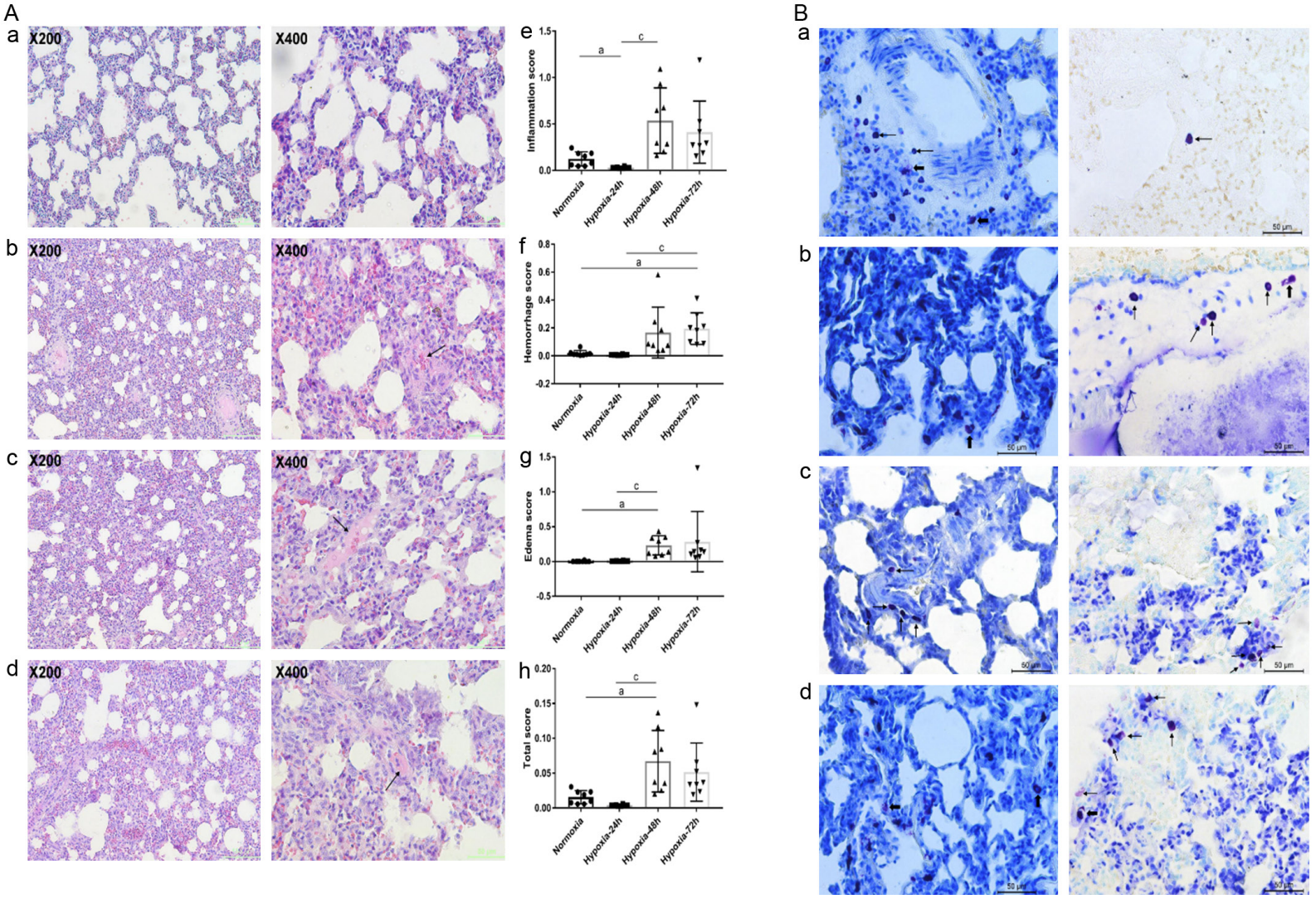
A
a
X200
X400
b
X200
X400
c
X200
X400
d
X200
X400
e
Inflammation score
Normoxia
Hypoxia-24h
Hypoxia-48h
Hypoxia-72h
f
Hemorrhage score
g
Edema score
h
Total score
B
a
b
c
d
50 μm

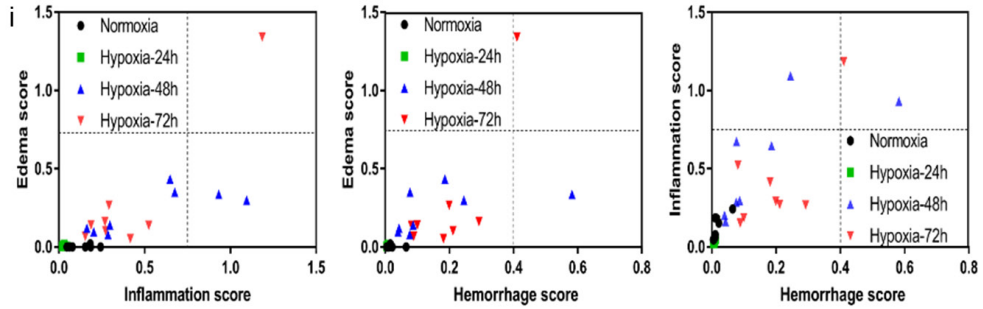

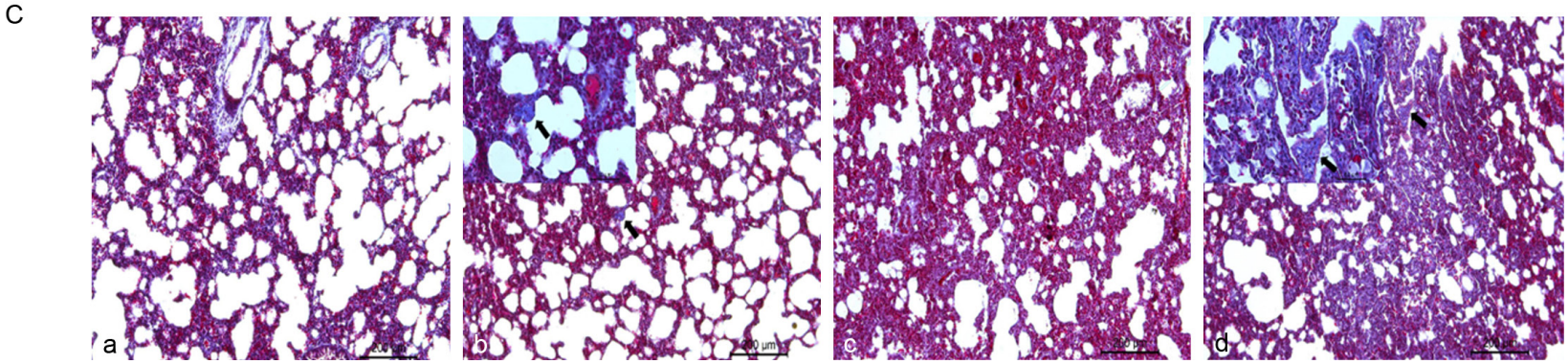

Figure 5. Pathological staining of lung tissue (× 200 and × 400). A. H&E staining of lung tissue in rats. a. Normoxic control group; b. Hypoxic 24-hour group; c. Hypoxic 48-hour group; d. Hypoxic 72-hour group; e. Inflammation score; f. Hemorrhage score; g. Edema score; h. Total score; i. Correlation of pathological score. Compared with the normoxic control group, $^{a}P < 0.05$, Compared with the hypoxic 24-hour group, $^{c}P < 0.05$. The arrows indicate alveolar or interstitial edema; B. Toluidine blue staining of lung tissue in rats (× 400). a. Normoxic control group; b. Hypoxic 24-hour group; c. Hypoxic 48-hour group; d. Hypoxic 72-hour group. The thin arrow indicates mast cells and the thick arrow indicates degranulation; C. Masson-Goldner trichrome staining of lung tissue in rats (× 100). a. Normoxic control group; b. Hypoxic 24-hour group; c. Hypoxic 48-hour group; d. Hypoxic 72-hour group. The arrows indicate pulmonary interstitial fibrosis, but the fibrosis was not obvious in each group.

Table 2. Comparison of MC quantity and degranulation rate in rat lung tissue (n = 10, $\bar{x}$ ± s)

Group	MC count (cells/HPF)	Degranulation rate (%)
Normoxic control group	2.10 ± 1.20	28.30 ± 39.90
Hypoxic 24-hour group	1.80 ± 1.03	46.70 ± 44.32
Hypoxic 48-hour group	4.00 ± 2.54[a,d]	63.30 ± 35.62[a]
Hypoxic 72-hour group	5.20 ± 1.75[b,d]	80.40 ± 21.18[b,c]

Compared with the normoxic control group, [a]P < 0.05, [b]P < 0.01; Compared with the hypoxic 24-hour group, [c]P < 0.05, [d]P < 0.01.

the hypoxic 24-hour group, the total score of the hypoxic 48-hour group was significantly increased (P < 0.01) (**Figure 5Ah**). As shown in **Figure 5Ai**, the inflammatory and edema scores were correlated in the hypoxic group at 48 and 72 hours (P < 0.05), but not in the normoxic control group or the hypoxic group at 24 hours. The hemorrhage and edema scores showed a correlation in the 72-hour hypoxic group (P < 0.05), but there was no correlation in the other groups. The hemorrhage and inflammation scores showed a correlation in the normoxic control group or the hypoxic 24- and 48-hour groups (P < 0.05), but there was no correlation in the hypoxic 72-hour group.

Mast cell degranulation releases histamine and trypsin, which increase pulmonary microvascular permeability [18] (**Figure 5B**). Toluidine blue staining showed that hypertrophic cell infiltration and degranulation occurred in both the normoxic control and the hypoxic exposure groups, scattered around pulmonary blood vessels or the interstitium. Under high magnification, the mast cell granules appeared purplish-red and the nuclei were blue. The intact cells had clear cytoplasms. The capsules of the degranulated cells were ruptured, and the granules gushed out of the cell membranes and gathered around the cell membranes. Compared with the normoxic control group, the mast cell count in the hypoxic 24-hour group decreased, but the degranulation rate increased, and the mast cell count in the hypoxic 48-hour and 72-hour groups showed a significant difference (P < 0.05). The degranulation rate of the mast cells was also significantly different (P < 0.05; P < 0.01). Compared with the hypoxic 24-hour group, the mast cell counts in the hypoxic 48-hour group and 72-hour group were different (P < 0.01), and the mast cell degranulation rate was also significantly different in the hypoxic 72-hour group (P < 0.05) (**Table 2**).

Masson staining confirmed that there was no obvious collagen deposition in the lung interstitium of the normoxic control group and the hypoxic exposure group, and there was occasional collagen fiber staining around the pulmonary blood vessels (**Figure 5C**).

Lung tissue occludin expression

Occludin is one of the major proteins in tight junctions, can reflect the tightness between alveolar epithelial cells and plays an important role in hypoxia-induced lung injury [19]. Our evaluation of protein expression by Western blotting revealed that occludin was strongly positively expressed in the normoxic control group, but it was relatively weakly expressed in the three hypoxic exposure groups (**Figure 6A**). The gray value analysis is shown in **Figure 6A**. Compared with the normoxic control group, the gray values in the 24- and 48-hour hypoxia groups were significantly lower (P < 0.05), and the gray values in the 72-hour hypoxia group were also significantly lower (P < 0.01). In the Hypoxic exposure group, the gray value of the 72-hour hypoxia group was significantly lower than it was in the 24-hour hypoxia group (P < 0.05). Immunohistochemistry revealed that the occludin expression was strongly positive in the normoxic control group, but the expression was weakly positive in the hypoxic exposure group (**Figure 6B**). The MOD analysis is shown in **Figure 6B**. Compared with the normoxic control group, the MOD in the 24-, 48-, and 72-hour hypoxia groups was significantly lower (P < 0.01).

Discussion

Studies have shown that excessive hypoxic pulmonary vasoconstriction (HPV) and hypoxic ventilatory response (HVR) are two characteristic changes in HAPE-susceptible individuals [13]. Pulmonary vasoconstriction is affected by pulmonary vascular smooth muscle and the vascular endothelium, lung volume, respiratory regulation, left ventricular end-diastolic pressure, and neurohumoural response. Continuous hypoxic conditions increase sympathetic vasoconstriction, reduce NO production, and increase vascular endothelin production [20]. The

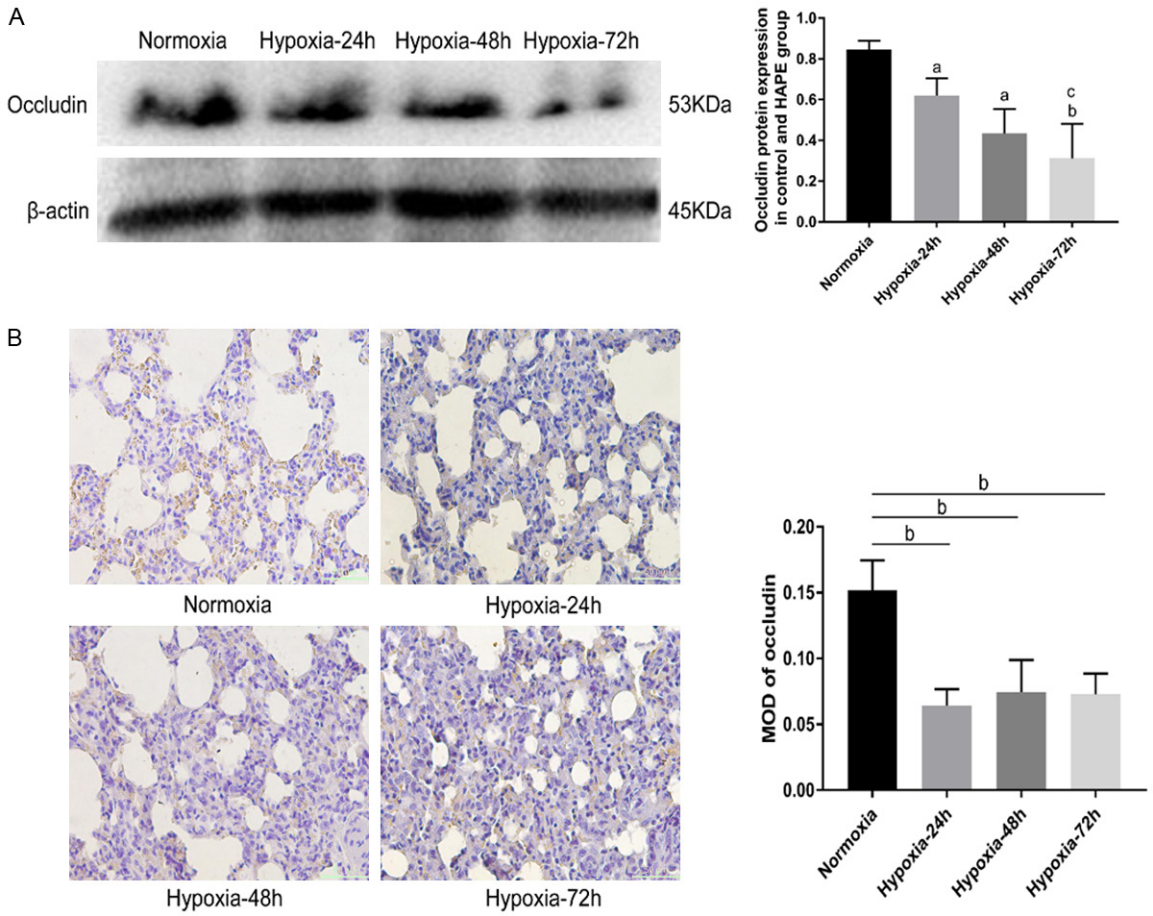

Figure 6. The expression of occludin in rat lung tissue is down-regulated over time. A. Evaluation of protein expression by Western blotting. B. Immunohistochemical observation of occludin expression in rat lung tissue (× 400). Compared with the normoxic control group, $^{a}P < 0.05$, $^{b}P < 0.01$; Compared with the hypoxic 24-hour group, $^{c}P < 0.05$.

former is an important vasodilator that relaxes vascular smooth muscle through the cGMP-PKG pathway, which is a strong vasoconstrictor [21]. The hypoxia-activated TGF-β signalling pathway regulates the synthesis of endothelin to cause pulmonary vascular smooth muscle contraction [22]. These factors are closely related to the formation of pulmonary hypertension. Excessive pulmonary arterial pressure impedes normal lung ventilation, and hypoventilation causes low PaO_2 in the alveoli, which further stimulates HPV and decreases the arterial blood PaO_2 [13]. In this experiment, rats in the high-altitude pulmonary edema group showed significant hypoxemia, and $PaCO_2$ decreased briefly in the 24-hour hypoxia group and then significantly increased in the 48- and 72-hour hypoxia groups. The pH value decreased after 24 and 48 hours under hypoxia. There was a temporary increase and a decrease in the 72-hour hypoxia group, indicating that in the early stages of treatment, the rats showed hyperventilation due to the decrease in blood pressure partial pressure, and then the reaction was weakened indirectly, indicating that the hypoxic exposure group were missing. The prolonged oxygen time increases the degree of hypoventilation. The concentrations of TCO_2, HCO_3 and BEecf in the hypoxic exposure group were lower than those in the normoxic control group, indicating that acidic metabolites in the blood of rats increased significantly with the time of hypoxia, which may be gradually increased. The ventilation response is related.

W/D is an indicator that assesses the severity of pulmonary edema, and the BALF protein is an indicator for evaluating the permeability of alveolar capillaries. In our study, the levels of

W/D and the BALF protein in the lung tissue of rats in the hypoxic exposure group were significantly higher than those in the normoxia control group, indicating that the alveolar capillary permeability of the rats in the hypoxic exposure group was enhanced. Studies have shown that hypoxia can promote the expressions of mRNA and the protein of angiogenesis-related factors, such as vascular endothelial growth factor (VEGF) and vascular endothelial growth factor receptor (VEGFR) [23]. In the rats with HAPE, the upregulation of VEGF expression in lung tissue activates angiogenesis-related signalling pathways, such as Notch, resulting in a series of cascades that promote angiogenesis, which is characterized by the high permeability of the alveolar capillary endothelium [24, 25]. This cascade can lead to the development of pulmonary edema, but the specific mechanism needs to be further studied in the HAPE model.

Unlike the severe inflammatory response of ARDS, the intensity of the inflammatory response in HAPE patients is diminished [26]. Clinical studies have shown that HAPE is a non-inflammatory destruction of the alveolar capillary barrier, which indicates that in the early stage of HAPE the levels of inflammatory factors such as IL-6 and TNF-α in BALF are normal or transiently elevated, and then return to normal levels, indicating that the inflammatory response is not a key trigger for HAPE, but a secondary change [26-30]. Related studies have shown that elevated levels of IL-6 and TNF-α in plasma and BALF in HAPE patients and animals may be associated with hypoxia-induced IL-6 expression [31]. IL-6 induces IL-6 involvement in hypoxia response through the hypoxia-mediated activation of the nuclear factor NF-IL-6 binding site, with TNF-α coordination involved in the above process [31]. Studies have also shown that single nucleotide polymorphisms (SNPs) in IL-6 are significantly associated with the risk of HAPE [32]. As an effective anti-inflammatory and immunosuppressive factor, IL-10 has been reported to promote the secretion of CD1dhiCD5+B cells by HIF-α, which regulates immune responses in autoimmune diseases. In the present study, IL-6 and TNF-α in plasma and BALF were significantly elevated after 24 hours of hypoxic exposure, peaked at 48 hours of hypoxic exposure, and then decreased after 72 hours of hypoxic exposure. It remained essentially unchanged, while IL-10 in plasma and BALF continued to increase after 24, 48, and 72 hours of continuous hypoxic exposure. This result indicates that during chronic hypoxic exposure, the rats were shown a degree of inflammatory response leading to a pro-inflammatory/anti-inflammatory imbalance, and over time, the inflammatory response tends to be gradual or diminished, and the results were consistent with most of the basic and clinical studies related to HAPE [26, 33].

Our results showed that typical pathological changes similar to HAPE could be observed 24 hours after hypoxic exposure, and lung injury was manifested as alveolar septal thickening, pulmonary interstitial edema, hemorrhage, inflammatory cell infiltration, etc. The results were consistent with those of c. Bai et al. [9]. However, for those susceptible to HAPE in the past, no residual pulmonary dysfunction was observed at rest or in a stable state, which may be related to the reduction or flattening of pathological changes [21]. After 72 hours of continuous hypoxic exposure, the score is reduced, and there is no significant difference between the two groups, which is similar to the pathological score of lung injury. At the same time, the correlation between the inflammation, edema and hemorrhage scores indicates that inflammation is not the initial factor causing pulmonary edema, but other factors lead to increased pulmonary microvascular permeability in the early stages of HAPE [30]. Studies have shown that IL-6, as a cytokine significantly induced by hypoxia, can also promote the survival and activation of mast cells under hypoxia conditions [34]. Mast cells have been shown to be involved in the effect of pulmonary microvessels in hypoxia, changing vascular permeability [35], and the release of histamine and other substances by degranulation has become one of the important causes of hypoxic pulmonary hypertension [36, 37]. In the present study, the mast cell count and the degranulation rate increased significantly 48 and 72 hours after hypoxic exposure, which may be associated with the increase in mast cell numbers and with the histamine release caused by prolonged chronic hypoxic exposure [36-38]. The specific functions and mechanisms of these factors need to be further studied and confirmed. It has been reported that ARDS can cause lung hyaline membrane lesions and pulmonary interstitial fibrosis within 24 hours, which is different from HAPE. Pulmonary interstitial fibrosis is not a characteristic pathological change

for HAPE [38-40]. Our results did not cause hyaline membrane changes or obvious pulmonary interstitial fibrosis, suggesting that the chronic hypoxic exposure in this study was not sufficient to confirm the early stages of ARDS development.

The mechanism of HAPE is a complex pathophysiological process. When the alveolar epithelial integrity is impaired, protein-rich edema fluid flows into the alveoli [41]. Occludin plays an important role in maintaining the integrity of the alveolar epithelium [42]. Studies have found that the expression level of occludin in the HAPE model is related to the stability of the alveolar-capillary barrier. As the expression of occludin increases, the stability of the alveolar-capillary barrier gradually increases [19]. This is in contrast to the low expression of occludin in the alveolar epithelium of rats in the hypoxic exposure group, while the W/D and LPI was significantly higher than that of the normoxic control group, and the lung histopathology shows that the alveolar epithelial integrity is destroyed, and the alveolar-capillary barrier function is consistently impaired. Therefore, the low expression of the tight junction-associated protein occludin in the alveolar epithelium may be another important factor in the production of HAPE.

In summary, after 24, 48, and 72 hours of hypoxic exposure, healthy rats were able to cause pulmonary edema without a non-exercise and endotoxin induction, which are all associated with HAPE after a rapid increase to a specific altitude and 2-4 days of plateau in susceptible populations and consistent with the pathological characteristics and pathophysiological changes of HAPE. Furthermore, in this study, the inflammatory evaluation index was not persistently high, and it may not be a key factor in the onset of pulmonary edema in rats, and it does not strongly confirm the development of ARDS during chronic hypoxic exposure.

Acknowledgements

This study was supported by the Tianjin Natural Science Foundation of China (15JCYBJC28500).

Disclosure of conflict of interest

None.

Address correspondence to: Hui Ding and Shike Hou, School of Disaster Medical Research, Tianjin University, Tianjin 300072, China. E-mail: huidingah@163.com (HD); houshike@126.com (SKH)

References

[1] Zafren K. Prevention of high altitude illness. Travel Med Infect Dis 2014; 12: 29-39.

[2] Qi Y, Sun J, Zhu T, Wang W, Liu J, Zhou W, Qiu C and Zhao D. Association of angiotensin-converting enzyme gene insertion/deletion polymorphism with high-altitude pulmonary oedema: a meta-analysis. JRAAS 2011; 12: 617-623.

[3] Sheppard RL, Swift JM, Hall A and Mahon RT. The influence of CO2 and exercise on hypobaric hypoxia induced pulmonary edema in rats. Front Physiol 2018; 9: 130.

[4] Li X, Jin T, Zhang M, Yang H, Huang X, Zhou X, Huang W, Qin L, Kang L, Fan M and Li S. Genome-wide association study of high-altitude pulmonary edema in a Han Chinese population. Oncotarget 2017; 8: 31568-31580.

[5] Maggiorini M. Prevention and treatment of high-altitude pulmonary edema. Prog Cardiovasc Dis 2010; 52: 500-506.

[6] He Y, Liu L, Xu P, He N, Yuan D, Kang L and Jin T. Association between single nucleotide polymorphisms in ADRB2, GNB3 and GSTP1 genes and high-altitude pulmonary edema (HAPE) in the Chinese Han population. Oncotarget 2017; 8: 18206-18212.

[7] Gupta RK, Soree P, Desiraju K, Agrawal A and Singh SB. Subclinical pulmonary dysfunction contributes to high altitude pulmonary edema susceptibility in healthy non-mountaineers. Sci Rep 2017; 7: 14892.

[8] Zhu L, Liu L, He X, Yan M, Du J, Yang H, Zhang Y, Yuan D and Jin T. Association between genetic polymorphism of telomere-associated gene ACYP2 and the risk of HAPE among the Chinese Han population: a case-control study. Medicine 2017; 96: e6504.

[9] Bai C, She J, Goolaerts A, Song Y, Shen C, Shen J and Hong Q. Stress failure plays a major role in the development of high-altitude pulmonary oedema in rats. Eur Respir J 2010; 35: 584-591.

[10] Kleinsasser A, Levin DL, Loeckinger A and Hopkins SR. A pig model of high altitude pulmonary edema. High Alt Med Biol 2003; 4: 465-474.

[11] Schoene RB and Goldberg S. The quest for an animal model of high altitude pulmonary edema. Int J Sports Med 1992; 13 Suppl 1: S59-61.

[12] Li S, Ran Y, Zhang D, Chen J, Li S and Zhu D. MicroRNA-138 plays a role in hypoxic pulmo-

nary vascular remodelling by targeting Mst1. Biochem J 2013; 452: 281-291.
[13] Hohenhaus E, Paul A, McCullough RE, Kücherer H and Bärtsch P. Ventilatory and pulmonary vascular response to hypoxia and susceptibility to high altitude pulmonary oedema. Eur Respir J 1995; 8: 1825-1833.
[14] Carpenter TC, Reeves JT and Durmowicz AG. Viral respiratory infection increases susceptibility of young rats to hypoxia-induced pulmonary edema. J Appl Physiol (1985) 1998; 84: 1048-1054.
[15] Bärtsch P. High altitude pulmonary edema. Respiration 1997; 64: 435-43.
[16] Bärtsch P and Swenson ER. Acute high-altitude illnesses. N Engl J Med 2013; 369: 1666-7.
[17] Smith KM, Mrozek JD, Simonton SC, Bing DR, Meyers PA, Connett JE and Mammel MC. Prolonged partial liquid ventilation using conventional and high-frequency ventilatory techniques: gas exchange and lung pathology in an animal model of respiratory distress syndrome. Crit Care Medicine 1997; 25: 1888-1897.
[18] Droma Y, Hanaoka M, Hotta J, Naramoto A, Koizumi T, Fujimoto K, Honda T, Kobayashi T, Kubo K. Pathological features of the lung in fatal high altitude pulmonary edema occurring at moderate altitude in Japan. High Alt Med Biol 2001; 2: 515-523.
[19] Zhou Q, Wang D, Liu Y, Yang X, Lucas R and Fischer B. Solnatide demonstrates profound therapeutic activity in a rat model of pulmonary edema induced by acute hypobaric hypoxia and exercise. Chest 2017; 151: 658-667.
[20] Swenson ER and Bartsch P. High-altitude pulmonary edema. Compr Physiol 2012; 2: 2753-2773.
[21] Beall CM, Laskowski D and Erzurum SC. Nitric oxide in adaptation to altitude. Free Radic Biol Med 2012; 52: 1123-1134.
[22] Olave N, Nicola T, Zhang W, Bulger A, James M, Oparil S, Chen YF and Ambalavanan N. Transforming growth factor-β regulates endothelin-1 signaling in the newborn mouse lung during hypoxia exposure. Am J Physiol Lung Cell Mol Physiol 2012; 302: L857-865.
[23] Huang SC, Rehman MU, Lan YF, Qiu G, Zhang H, Iqbal MK, Luo HQ, Mehmood K, Zhang LH and Li JK. Tibial dyschondroplasia is highly associated with suppression of tibial angiogenesis through regulating the HIF-1α/VEGF/VEGFR signaling pathway in chickens. Sci Rep 2017; 7: 9089.
[24] Zhao Q, Eichten A, Parveen A, Adler C, Huang Y, Wang W, Ding Y, Adler A, Nevins T, Ni M, Wei Y and Thurston G. Single-cell transcriptome analyses reveal endothelial cell heterogeneity in tumors and changes following antiangiogenic treatment. Cancer Res 2018; 78: 2370-2382.
[25] Tetzlaff F, Adam MG, Feldner A, Moll I, Menuchin A, Rodriguez-Vita J, Sprinzak D and Fischer A. MPDZ promotes DLL4-induced Notch signaling during angiogenesis. Elife 2018; 7.
[26] Kubo K, Hanaoka M, Hayano T, Miyahara T, Hachiya T, Hayasaka M, Koizumi T, Fujimoto K, Kobayashi T and Honda T. Inflammatory cytokines in BAL fluid and pulmonary hemodynamics in high-altitude pulmonary edema. Respir Physiol 1998; 111: 301-310.
[27] Swenson ER, Maggiorini M, Mongovin S, Gibbs JS, Greve I, Mairbaurl H and Bartsch P. Pathogenesis of high-altitude pulmonary edema: inflammation is not an etiologic factor. JAMA 2002; 287: 2228-2235.
[28] Kleger GR, Bartsch P, Vock P, Heilig B, Roberts LJ 2nd and Ballmer PE. Evidence against an increase in capillary permeability in subjects exposed to high altitude. J Appl Physiol (1985) 1996; 81: 1917-1923.
[29] Maggiorini M, Melot C, Pierre S, Pfeiffer F, Greve I, Sartori C, Lepori M, Hauser M, Scherrer U and Naeije R. High-altitude pulmonary edema is initially caused by an increase in capillary pressure. Circulation 2001; 103: 2078-2083.
[30] Pavlicek V, Marti HH, Grad S, Gibbs JS, Kol C, Wenger RH, Gassmann M, Kohl J, Maly FE, Oelz O, Koller EA and Schirlo C. Effects of hypobaric hypoxia on vascular endothelial growth factor and the acute phase response in subjects who are susceptible to high-altitude pulmonary oedema. Eur J Appl Physiol 2000; 81: 497-503.
[31] Yan SF, Tritto I, Pinsky D, Liao H, Huang J, Fuller G, Brett J, May L and Stern D. Induction of interleukin 6 (IL-6) by hypoxia in vascular cells. Central role of the binding site for nuclear factor-IL-6. J Biol Chem 1995; 270: 11463-11471.
[32] He X, Wang L, Zhu L, Yuan D, He Y and Jin T. A case-control study of the genetic polymorphism of IL6 and HAPE risk in a Chinese Han population. Clin Respir J 2018; 12: 2419-2425.
[33] Kubo K, Hanaoka M, Yamaguchi S, Hayano T, Hayasaka M, Koizumi T, Fujimoto K, Kobayashi T and Honda T. Cytokines in bronchoalveolar lavage fluid in patients with high altitude pulmonary oedema at moderate altitude in Japan. Thorax 1996; 51: 739-742.
[34] Gulliksson M, Carvalho RF, Ulleras E and Nilsson G. Mast cell survival and mediator secretion in response to hypoxia. PLoS One 2010; 5: e12360.
[35] Steiner DR, Gonzalez NC and Wood JG. Mast cells mediate the microvascular inflammatory response to systemic hypoxia. J Appl Physiol (1985) 2003; 94: 325-334.
[36] Kay JM, Waymire JC and Grover RF. Lung mast cell hyperplasia and pulmonary histamine-

forming capacity in hypoxic rats. Am J Physiol 1974; 226: 178-184.
[37] Haas F and Bergofsky EH. Role of the mast cell in the pulmonary pressor response to hypoxia. J Clin Invest 1972; 51: 3154-3162.
[38] Williams A, Heath D, Kay JM and Smith P. Lung mast cells in rats exposed to acute hypoxia, and chronic hypoxia with recovery. Thorax 1977; 32: 287-295.
[39] Chesnutt AN, Matthay MA, Tibayan FA and Clark JG. Early detection of type III procollagen peptide in acute lung injury. Pathogenetic and prognostic significance. Am J Respir Crit Care Med 1997; 156: 840-845.
[40] Wheeldon EB, Walker ME, Murphy DJ and Turner CR. Intratracheal aerosolization of endotoxin in the rat: a model of the adult respiratory distress syndrome (ARDS). Lab Anim 1992; 26: 29-37.
[41] Liu M, Gu C and Wang Y. Upregulation of the tight junction protein occludin: effects on ventilation-induced lung injury and mechanisms of action. BMC Pulm Med 2014; 14: 94.
[42] McNeil E, Capaldo CT and Macara IG. Zonula occludens-1 function in the assembly of tight junctions in Madin-Darby canine kidney epithelial cells. Mol Biol Cell 2006; 17: 1922-1932.